Clays and Clay Minerals, Vol. 52, No. 6, 767–778, 2004.

GREEN EARTH PIGMENT FROM THE KADAŇ REGION, CZECH REPUBLIC: USE OF RARE Fe-RICH SMECTITE

David Hradil[1,*], Tomáš Grygar[1], Michaela Hrušková[1], Petr Bezdička[1], Kamil Lang[1], Oldřich Schneeweiss[2] and Marek Chvátal[3]

[1] Institute of Inorganic Chemistry AS CR, 250 68 Řež, Czech Republic
[2] Institute of Physics of Materials AS CR, Žižkova 22, 616 62 Brno, Czech Republic
[3] Faculty of Sciences, Charles University, Albertov 6, 128 43 Prague 2, Czech Republic

Abstract—A collection of green earths belonging to traditional artists' pigments was examined in terms of mineralogy and provenance. The studied specimens included both mineralogical reference compounds and selected commercially available artists' pigments, and contained green micas (glauconite or celadonite), chlorite, or smectite as pigmenting agents. The samples were examined by X-ray diffraction, Mössbauer spectroscopy, infrared (IR) spectroscopy, ultraviolet-visible (UV-Vis)-near-IR diffuse-reflectance spectroscopy and voltammetry of microparticles. Particular attention was paid to the Kadaň green earth, mined until the 20th century in the West Bohemia deposit. The Greene-Kelly charge-reduction test, detailed description of non-basal diffraction patterns and characteristic vibrations in the mid-IR spectra were used to classify the major pigmenting agent of the Kadaň green earth as ferruginous smectite with separately diffracting saponite-like clusters. The smectite contains ~15% Fe, mainly in the trivalent form, a detectable fraction of Fe in tetrahedral sites, and it is accompanied by a significant amount of Ti-bearing relict minerals due to its volcanogenic origin. On the contrary, in green micas (glauconite and celadonite) the Ti content is much smaller. Diffuse reflectance spectroscopy was found suitable for distinguishing Fe as a constituent of free Fe oxides from Fe in the clay structure. It was also found to be useful for discriminating between green micas and smectites.

Key Words—Artists' Pigments, Celadonite, Ferruginous Smectite, Glauconite, Green Earths.

INTRODUCTION

Green earths, or green clayey materials containing Fe compounds as the pigmenting agents, have been used in fine art since ancient times and continue to be used (Grissom, 1986; Hradil *et al*., 2003). The minerals which are responsible for the color of green earths belong to four groups – (1) the clay micas celadonite and glauconite, (2) smectite minerals, (3) chlorites, and (4) serpentine minerals (Grissom, 1986). The mineralogical diversity of green earths exploited throughout history is hence rather broad, but mineralogical analysis of real paint layers is rare. This may be due to the limitations of analysis of rare, very small, and extremely heterogeneous samples of paint layers of art works. Fine-grained greenish layers in paintings often contain a mixture of earthy materials that cannot be easily interpreted in mineralogical terms. Sometimes, mono-mineral crystals of celadonite are easily recognizable as noticeable dark-green grains, and therefore celadonite is sometimes explicitly mentioned in the materials research reports. Light microscopy, which is commonly used in material studies of works of art, is usually only able to classify the pigment as green earths, particularly in cases when other greens are excluded by elemental analysis. Further differentiation was only rarely based on X-ray diffraction (XRD) measurements (Yamasaki and Emoto, 1979 – glauconite; Mosk, 1975 – cronstedtite). Recently, green earth has reportedly been identified by light microscopy combined with Raman spectroscopy (Daniila *et al*., 2002) but the actual green mineral has not been specified. The mineralogy of traditional green earths could be elucidated by a study of materials from the historical mining localities.

This work focuses on smectites from the historical source locality of green earth in Brodce near Kadaň in the Czech Republic. For comparison, samples were collected from the type localities of celadonite from Monte Baldo deposit near Verona, Italy, and sedimentary glauconite from Prague. In those localities, mining for fine-art purposes is well documented historically. The most famous locality for the bluish-green type of green earth in Europe, Monte Baldo, Italy, was mentioned as early as at 1574, originally as 'Veronese green earth', and it was mined until World War II. Another type locality of the Baroque period is the historical mining area near Kadaň in the Czech Republic, probably exploited since the 15th century with maximum production reached in the 18th and 19th centuries (Bláhová, 2002). Although the mine was closed soon after 1950, the term 'Bohemian green earth' still persists in modern commercial production. The same name has also been used for other, much less important green earths – glauconitic claystones mined

* E-mail address of corresponding author:
hradil@iic.cas.cz
DOI: 10.1346/CCMN.2004.0520612

near Hloubětín, Prague, from the 19th to the 20th century.

In this study, samples from several type localities were compared with reference clays and pigments in terms of their mineralogy, color and spectral properties. Near UV-Vis-near IR diffuse reflectance spectroscopy (DRS) was used to characterize green earths and detect possible admixtures of free ferric oxides. While DRS has already been used for analysis of Fe oxides in clayey materials (Malengreau *et al*., 1994; Scheinost *et al*., 1998), much less attention has been paid to characterization of Fe^{n+} in clay minerals, since until now only nontronite (Bonnin *et al*., 1985; Sherman and Vergo, 1988) and micas (Dyar, 2002) were examined. The Vis spectral study of green earths has thus far been limited to their general color evaluation (Grissom, 1986). However, the near UV-Vis-near IR spectral properties of Fe^{2+} and Fe^{3+} in clay minerals could be a valuable tool in gaining specific information on their structure and composition. For example, DRS should be able to detect tetrahedrally coordinated Fe^{3+} ions in the clay minerals structure (Bonnin *et al*., 1985). The speciation of Fe in clayey materials and discussion of their color was completed by detection of free Fe oxides by DRS, voltammetry of microparticles, and Mössbauer spectroscopy. Another goal of the work was to evaluate which techniques or characteristics can serve to discriminate between the individual green earths used in works of art.

EXPERIMENTAL

'Bohemian' green earth from Kadaň, Czech Republic

Samples of the 'Bohemian' green earth from Brodce near Kadaň were taken from the walls near the western end of a closed mine gallery in the Brodce village area. This gallery follows the sub-horizontal dark-green layer of altered basaltic tuffs of Oligocene/Miocene age (Albrecht *et al*., 1903). The easily recognizable layer is, in its best development, formed by large isometric dark phenocrysts, pseudomorphs after augite and biotite flakes encountered with a green-white matrix. Green earth is enclosed between more compact greyish argillized tuffs and limestones. All these altered materials and sediments belong to the ''Střezov'' volcano-sedimentary group of beds, which was developed in the first neo-volcanic stage on the slope of Doupovské Mts. volcano (Malkovský, 1985). The historical mining of green earth pigments in this locality was reported *e.g.* by Albrecht *et al*. (1903) or more recently in local sources by Bílek *et al*. (1976). Bláhová (2002) mentioned that the main and most attractive part of the gallery is closed and the currently accessible locality in Brodce is possibly not identical to the historical one.

One heterogeneous fragment of the material collected was used to prepare a thin-section (0.5 mm thick) suitable for light microscopy in reflected and transmitted light and for scanning electron microscopy (SEM) with elemental analysis via EDX. From the remaining material, some black phenocrysts were removed mechanically and analyzed separately. The rest was ground in an agate mortar and analyzed as a bulk sample. A separate portion of the material was disaggregated in distilled water and the <4 μm size fraction was separated by the sedimentation method. This <4 μm clay fraction was used to prepare oriented samples by the slow sedimentation of clay suspension on a glass slide, drying in air and further subjected to solvation in ethylene glycol and glycerol vapors (Moore and Reynolds, 1997).

Glauconite from Prague

A sample of marine sedimentary glauconite was collected from Vidoule, near Prague. The layer of greenish 'glauconitic' claystones, which were also used for painting (Zahálka, 1921), is ~0.5–1 m thick here and is Turonian in age (Bělohorské group of beds). The <4 μm size fraction was separated from the raw material by sedimentation as in the previous case.

Celadonite from Monte Baldo, Italy

A sample of the raw material was obtained from the Department of Geochemistry, Mineralogy and Mineral Resources of Charles University in Prague. The sample was a compact piece of bluish green color and fine grain size. Relict oval concretions of gray basaltic tuffs represent an original material exposed to the post-volcanic alteration process. Before analysis, the gray concretions were removed and the sample was homogenized in an agate mortar.

Reference clay minerals

The following clays from The Clay Minerals Society's Source Clays Repository (Purdue University, Indiana) were used as reference materials: Ca-Mg montmorillonite (STx-1), nontronites (NAu-1, NAu-2, NG-1), saponite (SapCa-1), illite (IMt-1), ferruginous smectite (SWa-1), and chlorite (CCa-2). Additionally, whitish specimens of montmorillonite clay from Lastovce deposit, Slovakia, were used. All these samples were studied in their 'as received' state, except NG-1. Before analysis, the <4 μm size fraction was separated from the NG-1 nontronitic sandstone by the sedimentation method.

The yellow-green bentonite from Rokle deposit, Czech Republic, representing the same age and natural genesis as the green earth from Brodce was collected and analyzed. The Brodce (green earth) and Rokle (bentonite) localities are in the same area (~5 km apart) and both represent altered tuffs of Oligocene/Miocene age, belonging to the 'Střezov' group of beds.

Green earths available as artists' pigments

Several green earths from current commercial production denoted as 'Veronese', 'Bohemian' and

https://doi.org/10.1346/CCMN.2004.0520612 Published online by Cambridge University Press

'Cyprus' were obtained from Kremer Pigmente (Farbmühle, 88317 Aichstetten/Allgäu, Germany). The pigments were first analyzed by powder XRD to evaluate their phase composition; only specimens free of obviously artificial additives were further studied. Celadonite from Cyprus (Kremer catalogue numbers 17400 and 17410) is the dominant pigment used in contemporary production of genuine artists' pigments throughout the world, as it represents the most attractive bluish variety of the green earth. 'Veronese' green earth (Kremer catalogue number 11010) contains relatively pure Fe-rich smectite.

ANALYTICAL METHODS

Elemental analysis

The chemical composition of samples was determined in the Laboratories of Geological Institutes, Charles University, Prague. Commercial, finely milled pigments were analyzed without any pre-treatment; in the case of raw materials the <4 μm clay fraction was used.

One thin-section of the raw 'Bohemian' green earth from Brodce was examined using a Philips XL30 CP scanning electron microscope without surface metallization under low air pressure with a Robinson detector of back-scattered electrons (RBS) in combination with an EDX detector of X-rays (acceleration voltage 25 kV).

Charge reduction – the Greene-Kelly test

The layer-charge reduction was performed according to Greene-Kelly (1953) by Li saturation followed by heating to 300ºC. The test was used to classify smectites present in Brodce green earth, the reference bentonite from Rokle, the montmorillonite from Lastovce, and in reference montmorillonite (STx-1), saponite (SapCa-2) and nontronite (NAu-2). Approximately 3 g of the clay fraction of each sample was transferred to a 250 mL flask and dispersed in 200 mL of 1 M LiCl solution. After 1 day of shaking, the suspension was left to sediment. The supernatant liquid was removed, and a further 200 mL portion of 1 M LiCl solution was added. This procedure was repeated three times, and then 200 mL of distilled water were added to the flask with clay. After 1 day of shaking, the sample was centrifuged (7 min at 9800 rpm) and the aqueous layer was removed. The procedure was repeated until the supernatant liquid was free of chlorides ($AgNO_3$ test). Finally, the clay was dried at 60ºC; oriented samples were prepared by a slow sedimentation of the suspension on a fused silica glass, and subjected to XRD. The XRD patterns of air-dried, ethylene glycol and glycerol-solvated samples were taken before and after their 1 day of heating to 300ºC.

Phase analysis

The bulk geological and commercial pigments as well as the oriented clay fraction samples and Li-exchanged samples were analyzed by powder XRD using a Siemens D-5005 diffractometer with CuKα radiation, 45 mA, 40 kV and secondary monochromator. Slow scans in the 2θ angle region 60–77º were additionally performed using a Philips X'Pert PRO diffractometer with an X'Celerator detector with CoKα radiation, at 45 mA and 30 kV to distinguish non-basal 060 diffractions of individual clay minerals (Moore and Reynolds, 1997).

Optical properties of individual mineral grains in the thin-section of the Brodce green earth were examined using an Olympus BX40 microscope with transmitted polarized light.

Infrared spectroscopy

Selected Li-saturated samples were pressed with KBr (0.5 mg sample per 200 mg KBr) to 13 mm pellets. To remove physically sorbed water, the pellets were dried overnight at a temperature of 150ºC and after drying they were stored in a desiccator. The FTIR spectra were obtained using a Nicolet Magna 750 FTIR spectrometer with an IR source, KBr beam splitter, and DTGS KBr detector for the mid-IR region. Repeated scans (128) were accumulated for each sample at a resolution of 4 cm^{-1}. The spectra were interpreted according to Cracium (1986), Madejová *et al*. (1994), Vantelon *et al*. (2001), Madejová and Komadel (2001) and Bishop *et al*. (2002).

Diffuse reflectance spectroscopy, electrochemical analysis, and Mössbauer spectroscopy

The diffuse reflectance spectra were obtained using a UV/Vis Perkin Elmer Lambda 35 spectrometer equipped with an integrating sphere accessory Labs sphere RSA-PE-20. The samples were ground in an agate mortar and placed in 2 mm quartz cells before measurement. A $BaSO_4$ pellet was used as a white reference. The reflection spectra were acquired with the 0.5 nm step, converted to the K-M scale, smoothed by 7-point Fourier filter, and then deconvoluted into a set of Gaussian components using the peak-fitting module in *OriginPro 7.0* (OriginLab Corporation). The position of the respective components was estimated using the 2nd derivation of the spectra. The spectra were interpreted according to Sherman (1985, 1987), Sherman and Waite (1985), Malengreau *et al*. (1994), Scheinost *et al*. (1998) and Dyar (2002).

The voltammetric detection of Fe oxides was described in our previous reports (Grygar and van Oorschot, 2002; Grygar *et al*., 2002, 2003a). The detection limits of free ferric oxides by voltammetry and DRS (0.1–1%) are better than that of powder XRD, especially in more complex mineral mixtures and with poorly crystalline oxides. The most efficient identification tool is the combination of voltammetry and DRS (Grygar *et al*., 2003a).

Mössbauer spectroscopy was performed in transmission mode with a ^{57}Co source, cryostat (APD Cryogenics

https://doi.org/10.1346/CCMN.2004.0520612 Published online by Cambridge University Press

Table 1. The list of green earths and reference samples. Pigments obtained from Kremer Pigmente are denoted by K and the catalogue number.

Name	Description, color, mineral type	Origin, supplier
Mte Baldo	Raw material of historical Veronese green earth – celadonite	Mte Baldo near Verona, Italy
Vidoule	Raw green claystone – glauconite	Vidoule in Prague, CR*
Brodce	Raw material of historical Bohemian green earth – smectites	Brodce near Kadaň, CR, mine gallery
Rokle	Raw yellow-green bentonite – smectites	Rokle near Kadaň, CR, open quarry
Lastovce	Raw bentonite, white	Lastovce, Slovakia
K11010 Verona	Commercial 'Veronese green earth' – Fe-rich smectite	Kremer Pigmente
K17400 Cyprus	Commercial 'Cyprus green earth' – celadonite	Kremer Pigmente
K17410 Cyprus	Commercial 'Cyprus green earth' – celadonite	Kremer Pigmente
STx-1	Ca-Mg montmorillonite, white	Source Clays Repository†
NAu-1	Nontronite, green	Source Clays Repository
NAu-2	Nontronite, brown	Source Clays Repository
NG-1	Nontronite-rich sandstone, yellow-green	Source Clays Repository
SWa-1	Ferruginous smectite	Source Clays Repository
IMt-1	Illite	Source Clays Repository
SapCa-1	Saponite	Source Clays Repository
CCa-1	Mg-rich chlorite – ripidolite	Source Clays Repository

* CR: Czech Republic
† from The Clay Minerals Society's Source Clays Repository, Purdue University, Indiana

Inc.) for measurement at 20 K, amplifier (Ortec, Perkin Elmer), and a proportional counter. The results were compared to the reports by Murad and Wagner (1994) and Koester *et al*. (1999).

RESULTS

Mineralogical classification of samples

The list of samples of green earths, reference clay minerals, and artists' pigments studied and their brief mineralogical description is given in Table 1. X-ray diffraction is sufficient to identify the basic mineralogical types of green earths. The only difficulty, that of distinguishing between celadonite and glauconite, can be resolved when these minerals are present in sufficient amounts and their non-basal 060 reflections are clearly visible. As a function of octahedral Fe^{3+} content, the d_{060} XRD line lies slightly above 1.51 Å in the case of glauconite and slightly below this value in the case of celadonite (Odom, 1984). More detailed results of the mineralogical and elemental analysis of selected samples are summarized in Tables 2 and 3.

The raw material of the Brodce green earth is very heterogeneous. Its color varies from light or grayish green to brown-green and dark brown. The reddish brown color is imparted by the presence of free ferric oxides. The nicest variety of olive green color can be prepared by milling of spotted stone with black isometric phenocrysts and white-green clay matrix. That material was further examined because the original pigment was prepared by grinding the raw materials without separation.

Based on the results of the powder XRD, polarized light microscopy, and EDX analysis, the black insets contained mainly titanomagnetite of an approximate composition $Fe_{2.5}Ti_{0.5}O_4$, pseudomorphs after augite are filled by neo-formed smectite. The relict titanomagnetite and pseudomorphs after augite were not visible in the rocks lying below and above the green earth bed; only

Table 2. Mineralogical compositions of the samples studied.

Name	Clay minerals	Further minerals
Green earths from historical localities		
Mte Baldo, Italy	Celadonite	
Brodce, Czech Rep.	Fe-rich dioctahedral smectite, saponite, celadonite??? (very small amount)	Anatase, quartz, titanomagnetite, biotite
Vidoule, Czech Rep.	Glauconite, kaolinite, illite	Quartz
Reference bentonites		
Rokle, Czech Rep.	Fe-rich dioctahedral smectite	Anatase, quartz, biotite
Lastovce, Slovakia	Ca/Mg montmorillonite	
Commercial real green earth pigments, Kremer Pigmente		
11010 Veronese GE	Fe-rich dioctahedral smectite	Plagioclase
17400 Cyprus GE	Celadonite, smectite (very small amount)	Plagioclase
17410 Cyprus GE	Celadonite, smectite (very small amount)	Plagioclase

https://doi.org/10.1346/CCMN.2004.0520612 Published online by Cambridge University Press

Table 3. Chemical composition (wt.%) of green earths. Commercially available pigments are denoted by K with the Kremer catalogue number.

	Mica minerals				Smectites		
	Mte Baldo	Vidoule (<4 μm)	K17410	K17400	Brodce (<4 μm)	Rokle (<4 μm)	K11010
SiO_2	55.22	48.38	52.90	52.38	42.80	45.81	51.12
TiO_2	0.19	0.57	0.19	0.09	2.16	3.06	1.81
Al_2O_3	2.53	20.75	3.60	3.28	10.60	15.43	14.81
Fe_2O_3	16.86	9.72	18.57	18.29	14.22	8.51	9.38
FeO	3.30	0.51	1.83	1.31	0.73	0.12	1.17
MnO	0.01	0.01	0.09	0.07	0.02	0.01	0.10
MgO	5.51	1.85	5.40	6.27	6.18	2.62	2.71
CaO	0.36	1.02	0.98	1.58	3.09	3.51	5.82
Na_2O	0.26	0.08	0.19	0.12	0.26	0.15	2.70
K_2O	8.72	4.71	7.36	6.89	1.56	0.76	1.95
P_2O_5	0.10	0.86	0.11	0.47	0.62	0.94	0.55
H_2O^-	1.32	1.80	2.66	2.18	10.36	11.40	4.24
H_2O^+	4.43	8.41	5.04	4.92	6.34	6.85	3.15
CO_2	0.80	0.77	0.70	1.71	0.74	0.65	0.43
Total	99.61	99.44	99.62	99.56	99.68	99.82	99.94

biotite flakes are common in all these tuffs. Similarly, only biotite relics were found in the raw yellow-green bentonite from the Rokle deposit. In spite of the close proximity of the Rokle and Brodce deposits, the composition of the original volcanogenic material was different. The genesis of the green earth by sub-aquatic alteration of unusual augite-rich tuffs was mentioned by Albrecht *et al*. (1903).

Grain-like pseudomorphs are mostly filled with a fine-grained altered material with variable chemical composition. Relict biotite flakes are relatively depleted in K and, to the contrary, intense green weathering rims surrounding grains are enriched in this element (Figure 1). According to XRD, the clay fraction mainly contains smectite-group minerals in all altered material, accompanied by a detectable amount of anatase. No other clay minerals are present in the clay fraction. Micas (biotite, possibly celadonite) are identified only in the untreated raw material. The inter-granular matrix contains cream-white calcite fillings.

Predominant smectites can be sub-divided according to d_{060} spacing (*e.g.* Moore and Reynolds, 1997; Środoń *et al*., 2001), behavior in the Greene-Kelly test (Greene-Kelly, 1953), and the direct spectroscopic crystallochemical measurements of octahedral and tetrahedral sites occupancies (*e.g.* Madejová *et al*., 1994; Vantelon *et al*., 2001). The results of slow XRD scans of non-oriented clay fractions show two distinct d_{060} spacings of 1.505 and 1.532 Å, indicating the presence of one dioctahedral and one trioctahedral smectite structure, respectively (Figure 2). The slight increase in typical 'montmorillonite' spacing from d_{060} = 1.50 Å to 1.52 Å (typical nontronite) can be correlated directly with the increasing Fe^{3+} (or bulk Fe) content in the octahedral sheet (Koester *et al*., 1999). The diffraction at d_{060} = 1.53 Å appears in trioctahedral structures of saponites

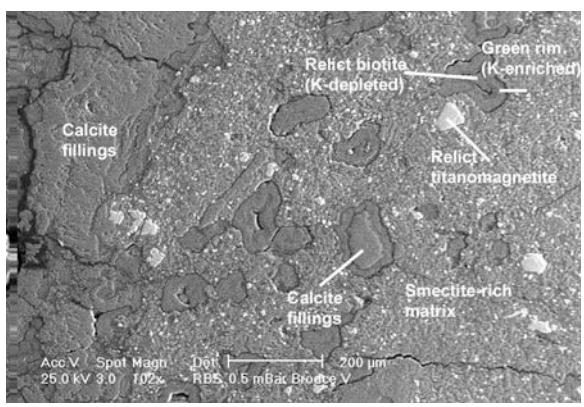

Figure 1. SEM image of the thin-section of the green earth from Brodce near Kadaň.

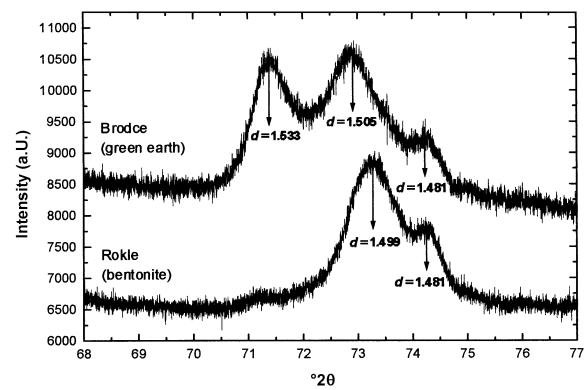

Figure 2. Non-basal d_{060} spacings of the Kadaň area smectites. The presence of saponite (d = 1.533) and dioctahedral Fe-rich smectite (d = 1.505) in Brodce green earth and montmorillonite (d = 1.499) in Rokle bentonite is indicated.

https://doi.org/10.1346/CCMN.2004.0520612 Published online by Cambridge University Press

with Mg^{2+} ions (Środoń *et al*., 2001) and in the reduced nontronites with Fe^{2+} ions in the octahedral sheet (Manceau *et al*., 2000). This diffraction peak d = 1.532 Å in the Brodce sample, similar to reference saponite SapCa-2, is only present within the green-earth strata; it is missing in other altered tuffs, *e.g.* from the Rokle deposit (Figure 2). This correlates with the much larger Mg content in the Brodce green earth as compared with the Rokle bentonite (Table 3).

The heating of Li-saturated samples should cause charge reduction in octahedral sheets and, therefore, the loss of expandability in the case of pure montmorillonites. Some difficulties may occur if mixtures of different smectites having both octahedral and tetrahedral charge of different magnitudes are present (Malla and Douglas, 1987). In the case of the Brodce green earth, the effect of the charge reduction was not observed. After the Greene-Kelly test, the sample expanded with ethylene glycol to d_{001} ≈17.0 Å and with glycerol to d_{001} ≈17.7 Å (Figure 3). This behavior was the same as for the reference nontronite (NAu-2) and saponite (SapCa-1) subjected to the same treatment. The reference Li-saturated montmorillonite (STx-1) did not expand, having d_{001} ≈9.8 Å. After Li saturation and heating, sufficient residual layer charge remained for the expansion of the Brodce green earth. The behavior of the Rokle bentonite is similar to the Brodce green earth but the expansion is somewhat reduced after the Greene-Kelly test. Basal spacing of d_{001} ≈ 16.7 Å could indicate some non-expanding layers within its structure.

The Brodce green earth is hence a mixture of dioctahedral Fe-rich smectites, which are not true nontronites, with separately diffracting trioctahedral clusters that are Mg-rich and saponite-like. The important question as regards smectite classification is the Fe distribution within these clay structures.

IR spectroscopy of the Brodce and Rokle smectites

Mineralogical classification of colored smectites from the Kadaň area (Brodce, Rokle) was checked by the examination of the stretching and bending vibrations

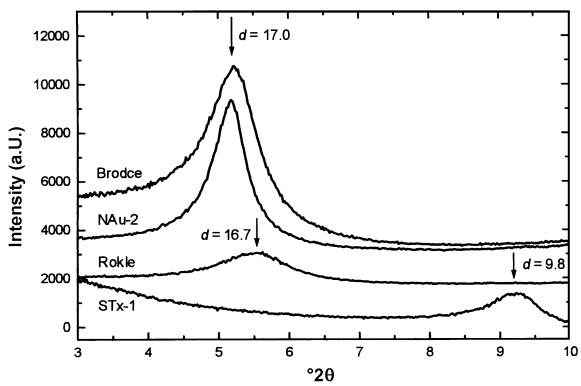

Figure 3. Basal diffractions of Li-saturated samples after the Greene-Kelly test and ethylene glycol solvation.

in their mid-IR (MIR) spectra. According to Madejová *et al*. (1994), Keeling *et al*. (2000), Vantelon *et al*. (2001), Madejová and Komadel (2001), Bishop *et al*. (2002), Fialips *et al*. (2002), Frost *et al*. (2002) and Gates (in press), the bending vibrations are used to distinguish the occupancy of the octahedral sites in montmorillonites, ferruginous smectites and nontronites. The list of vibrations described is given in Table 4; the OH-bending and lattice-deformation region of IR spectra are shown in Figure 4.

When the IR spectra of the samples are compared to reference clay minerals, some similarities with both nontronite NAu-2 and montmorillonite STx-1 are found. In the octahedral region, the band indicating Al–Al–OH-bending vibration at 915 cm^{-1} is visible, but it is less intense than in the case of pure montmorillonite. The Al–Fe^{3+}–OH-bending vibration occurs at 874 cm^{-1}, but the Fe^{3+}–Fe^{3+}–OH-bending vibration at 822 cm^{-1}, which is typical of true nontronites, is not visible in either the Brodce or the Rokle sample. The band near 840 cm^{-1} is not so determinative as it occurs in both montmorillonites (as Al–Mg–OH vibration, *e.g.* Cracium, 1984) and nontronites (as second Fe^{3+}–Fe^{3+}–OH vibration, *e.g.* Keeling *et al*., 2000).

In montmorillonites and ferruginous smectites, the position and intensity of this band is related to the relative Mg content (Gates, in press). Based on the fact that the band at 836 cm^{-1} is missing in the Rokle bentonite with 2.5 wt.% of Mg (Table 3) and clearly visible in the Brodce green earth with 6.3 wt.% of Mg (Table 3), its assignment as an Al–Mg–OH vibration seems appropriate. According to data presented by Gates (in press), the assignment of this band to Fe^{3+}–Fe^{3+}–OH is also unlikely as there is no band near 820 cm^{-1} in either sample. The Fe–O out-of- plane vibration is clearly visible in NAu-2 nontronite (at 678 cm^{-1}) and the Brodce green-earth sample (at 682 cm^{-1}). Lattice-deformation bands assigned by Madejová and Komadel (2001) as coupled Si–O and M–O out-of-plane vibrations appear at 628 cm^{-1} in the STx-1 montmorillonite, where M = Al and at 593 cm^{-1} in the case of NAu-2 nontronite, where M = Fe. In the Rokle bentonite and the Brodce green earth samples, this vibration is scarcely discernible; only a low-intensity peak appears near 605 cm^{-1} (Table 4).

In agreement with Goodman *et al*. (1976), the bands between 487 and 522 cm^{-1} (Si–O–Al vibration in montmorillonites), and 456–469 cm^{-1} (Si–O–Si vibration in montmorillonites) show a systematic shift to lower wavenumbers as the nontronitic character of the smectites increases, *i.e.* in the order STx-1 montmorillonite – Rokle bentonite – Brodce green earth – NAu-2 nontronite (Table 4).

The interpretation of the OH-stretching region is more difficult because of the interference of individual component bands; the approximate positions of different cation pairs are listed, *e.g.* in Madejová *et al*. (1994).

https://doi.org/10.1346/CCMN.2004.0520612 Published online by Cambridge University Press

Table 4. Characteristic vibrations in the mid-IR spectra of the Brodce green earth, Rokle bentonite and reference montmorillonite (STx-1) and nontronite (NAu-2), respectively.

	STx-1 montmorillonite	Rokle bentonite	Brodce green earth	NAu-2 nontronite
OH-bending bands (cm^{-1})				
Al–Al–OH	915	915	unclear	missing
Al–Fe–OH	missing	875	874	872
Al–Mg–OH, second Fe–Fe–OH	846	missing	836	839
Fe–Fe–OH	missing	missing	missing	822
Al–Mg–OH, Fe–Mg–OH, Si–O amorph.	794	broad (~796)	unclear	790
Lattice-deformation bands (cm^{-1})				
M–O out of plane	missing	broad (~700)	682	678
Coupled Si–O and *M*–O out of plane	628	unclear	unclear	poor (~593)
Al–O–Si	520	522	512	495
Si–O–Si	470	468	461	435
OH-stretching bands – appoximate positions of individual cation pairs (bands with discernible maxima are shown by their positions, those hidden in a broad interference band are indicated by +)				
Al–Al–OH	3629	3629, 3620	3629	3615
Al–Mg–OH	+	+	3603	+
Al–Fe–OH	missing	+	+	3580
Fe–Mg–OH	missing	missing	3570	+
Fe–Fe–OH	missing	missing	+	+

The Al–Al–OH vibrations appear in all cases at ~3620 and/or 3629 cm^{-1}, respectively. The Al–Mg–OH vibration is most intense in the case of the Brodce green earth (at 3603 cm^{-1}), in other cases is possibly hidden in a broad interference band. The Al–Fe–OH is intense in NAu-2 nontronite, missing in STx-1 montmorillonite and present in both the Brodce and Rokle samples. The Fe–Mg–OH vibration is missing in STx-1 montmorillonite and also Rokle bentonite, in Brodce green earth a local maximum at 3570 cm^{-1} is clearly discernible. In NAu-2 nontronite this vibration is less intense and hidden in a broad band. The Fe–Fe–OH vibration near 3550 cm^{-1} may be present only in NAu-2 nontronite and Brodce green-earth samples.

According to IR spectroscopy and to the results of the Greene-Kelly test, the Brodce green earth is a material resembling ferruginous smectite and the Rokle bentonite is closer to an Fe-rich montmorillonite. In the Brodce green earth, the larger octahedral Mg content is indicated particularly by intense OH-stretching vibrations of AlMg and FeMg cation pairs.

Spectral methods for speciation of Fe^{n+}

The color of green earths is affected by several d-d ligand-field and intervalence charge-transfer (IVCT) transitions in the visible region. Their denotation (capital letters) and identification are summarized in Table 5 and shown in Figure 5. All these transitions are superimposed on strong metal-to-ion charge-transfer (CT) transitions in the near-UV region, some are overlapped, and some have small absorption coefficients. The observable absorption bands are denoted by Roman

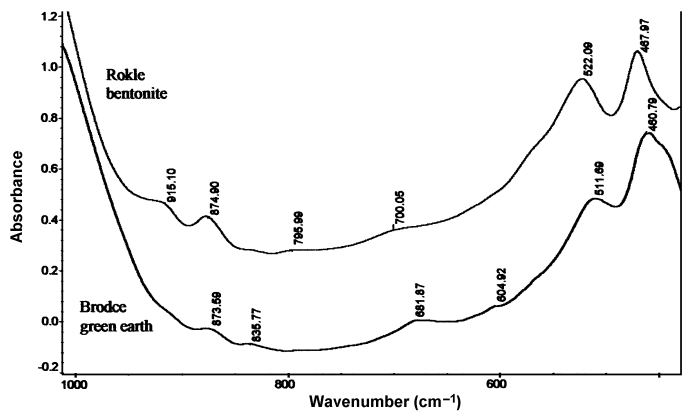

Figure 4. OH-bending and lattice-deformation region of the mid-IR spectra of Rokle bentonite and Brodce green earth sample.

https://doi.org/10.1346/CCMN.2004.0520612 Published online by Cambridge University Press

Table 5. Absorbing transitions in green earths and selected free Fe oxides.

Transition denotation	Absorbing species/transition	Wavelength of the maximum
A	Fe^{2+}	~9300 cm^{-1}
B	Fe^{3+}_{octa}	9100–11800 cm^{-1}
C	Fe^{2+}	~11360 cm^{-1}
D	Fe^{2+}-Fe^{3+} IVCT?	13300–18520 cm^{-1}
E	Fe^{3+}_{octa}, $^4T_2(^4G)$, (?) Fe^{3+}_{tetra}	13500–16130 cm^{-1}
F	Fe^{3+}, EPT, hematite	17700–19190 cm^{-1}
G	Fe^{3+}_{tetra}, $^4T_2(^4G)$	18520–20410 cm^{-1}
H	Fe^{3+}, EPT, goethite	20400–20800 cm^{-1}
I	Fe^{3+}, EPT, ferrihydrite	20400 cm^{-1}
J	Fe^{3+}_{octa}, ^4E,$^4A_1(^4G)$	21740–23800 cm^{-1}
K	Fe^{3+}_{tetra}, ^4E,$^4A_1(^4G)$, $^4T_2(^4D)$	21740–25000 cm^{-1}

Abbreviations: tetra – tetrahedral coordination, octa – octahedral coordination, EPT – electron-pair transition, CT – charge-transfer transition, IVCT – intervalence charge-transfer transition. Transitions are denoted according to Sherman (1985, 1987), Lear and Stucki (1987), Komadel *et al*. (1990), Malengreau *et al*. (1994), Scheinost *et al*. (1998) and Dyar (2002).

numerals and listed in Table 6. Sometimes the assignment of the bands to the transitions is not straightforward. For example, the transition D sometimes denoted Fe^{2+}-Fe^{3+} IVCT (Sherman, 1984; Lear and Stucki, 1987; Komadel *et al*., 1990; Dyar, 2002) falls into the range given by Sherman (1987) for the transition E of octahedral Fe^{3+}, and so the data interpretation was supported by the search for a correlation between the content of the chromophors (Fe^{2+}, Fe^{3+}) and the intensity of the individual bands. The identification of band V as transition G is also non-trivial. The band occurs at ~20,000 cm^{-1}, *i.e.* very close to the relatively strong transitions of magnetically interacting Fe^{3+}_{octa} ions in free ferric oxides (Malengreau *et al*., 1994; Scheinost *et al*., 1998, transitions F, H, I in Table 5). Fortunately, the band V can be found even in the presence of free ferric oxides goethite and hematite using the 2nd derivatives of the spectra (Grygar *et al*., 2003a).

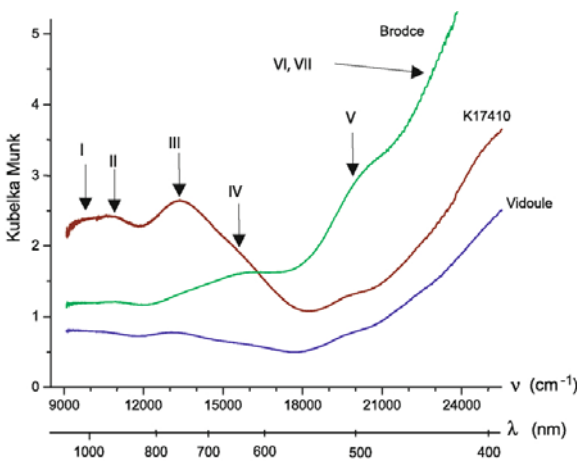

Figure 5. The appearance of the diffuse reflectance spectra of three clay minerals studied: smectite (Brodce), glauconite (Vidoule) and celadonite (K17410) with the bands of Fe^{n+} ions in the clay mineral structure assigned in Roman numerals (Table 6).

Statistically significant correlations between the integral intensities of the absorption bands and contents of Fe^{2+} and Fe^{3+} are shown in Table 6. The correlation proves unequivocally that band III is either IVCT or possibly Fe^{2+} transition, but certainly not the transition E of Fe^{3+}_{octa}. The lack of a correlation between bands V and VII and Fe^{2+} or Fe^{3+} content indicates that these bands can be attributed to some minor Fe species, probably to Fe^{3+}_{tetra}, expected to absorb at this wavenumber (Bonnin *et al*., 1985; Dyar, 2002). To support this interpretation, the presence of free ferric oxides was to be excluded as their absorption occurs at similar wavenubers (Table 5). The absence of Fe oxides in the Rokle <4 μm specimen exhibiting band V was proven by low-temperature Mössbauer spectroscopy and voltammetry of microparticles. In the majority of the clay mineral samples, band V is negligible or missing. In Figure 6, the integral intensity of band V is plotted against the total Fe content. The band is most intensive in brown smectite NAu-2, which is known to contain ~10% of Fe in the tetrahedral environment, and less intensive in NG-1 nontronite (<4 μm) with ~15% of Fe^{3+}_{tetra} (Gates *et al*., 2002), in commercially available 'Veronese' green earth (Kremer catalogue number 11010), and in greenish altered tuffs from Rokle and Brodce. Hence the clay component of the Brodce green earth contains some Fe^{3+} in tetrahedral sheets.

The relative intensities of band V are probably not directly proportional to the total amount of structural Fe^{3+}_{tetra} given by Gates *et al*. (2002) especially in the reference sample NG-1 (<4 μm) because of impurities. The admixture of a maghemite-like mineral also contains Fe^{3+}_{tetra}. The 2nd derivative of the spectra of NAu-2 contained a rather narrow band at 19,100 cm^{-1} (FWHM ~1000 cm^{-1}) overlapped with band V at 19,700 cm^{-1} (FWHM ~3500 cm^{-1}). On the contrary,

https://doi.org/10.1346/CCMN.2004.0520612 Published online by Cambridge University Press

Table 6. Results of the deconvolution of the DRS bands of Fe^{n+} ions in clay minerals studied: band numbering I–VII, their positions (mean, s.d. – standard deviation, n – number of specimens exhibiting the band), correlation coefficients of the integral intensities of the bands and the Fe^{2+} and Fe^{3+} contents in clay minerals, critical value of the correlation coefficient (at P = 95% for a given n), and the identification of the band (Table 5).

	Mean (cm^{-1})	s.d. (cm^{-1})	n	r^2 *vs.* Fe^{II}	r^2 *vs.* Fe^{III}	r^2_{CRIT}	Band
I	9295	184	8	0.8106	−0.0085	0.3994	A
II	10777	185	14	−0.1043	0.4842	0.2470	B
III	13244	140	8	0.7608	−0.1152	0.3994	D
IV	15560	196	14	−0.3949	0.5779	0.2470	E
V	19890	239	12	−0.3995	0.2210	0.2830	G
VI	22163	436	12	−0.7614	0.6369	0.2830	J
VII	24342	270	11	0.0143	−0.0441	0.3058	K

in the Brodce sample (<4 μm) there is a single minimum in the 2nd derivative of the spectra between 19,000 and 22,000 cm^{-1}.

To support the assignment of band V to Fe^{3+}_{tetra}, we followed the Mössbauer data processing used by Koester *et al*. (1999), who supposed that the paramagnetic doublets of Fe^{3+}_{tetra} and Fe^{3+}_{octa} have slightly different quadrupole splitting (Table 7). However, our results, obtained from samples NAu-1, NAu-2, NG-1 (<4 μm) and Rokle (<4 μm), did not permit such interpretation, probably because the difference in the quadrupole splitting is too small, and the sample mineralogy is too complex (NG-1). Mössbauer spectroscopy, however, proved the presence of traces of goethite in NAu-1 and NAu-2 (~4% of total Fe in partly collapsed sextets with hyperfine fields of units of T), and revealed a complex composition of NG-1 (<4 μm) with unassigned signals probably of superparamagnetic (nanocrystaline) oxides. The fraction of magnetically ordered Fe^{3+} remained constant in low-temperature measurement (Table 7). The dominant doublet in Mössbauer spectra corresponds to paramagnetic octahedral Fe^{3+} with parameters typical of nontronites (Koester *et al*., 1999) and illites (Murad and Wagner, 1994) and in the Rokle sample two minor doublets of paramagnetic Fe^{2+} appeared with parameters similar to Fe^{2+} in illite (Murad and Wagner, 1994).

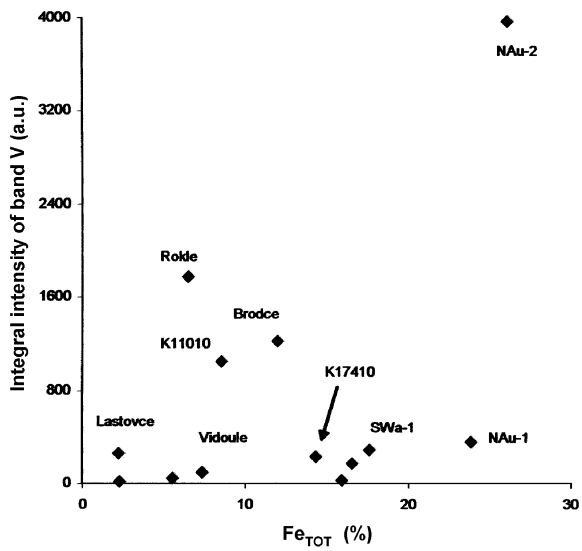

Figure 6. The plot of the integral intensity of band V *vs*. the total Fe percentage in the samples.

DISCUSSION

Powder XRD measurements clearly showed that the historical names (trademarks) of currently available pigments have no direct relation to the mineralogical composition of the earth materials from the historical localities. The blue-green sample from the Mte Baldo deposit near Verona, Italy, obtained from the mineralogical collection, was undoubtedly identified as pure celadonite with the d_{001} spacing at 9.9 Å and non-basal d_{060} spacing at 1.508 Å. However, the commercially available artists' pigment denoted as 'Veronese' green earth (Kremer catalogue number 11010) was in fact smectite with the basal d_{001} spacing at 15.0 Å and with a minor admixture of micas.

The 'Bohemian' green earth from Kadaň is traditionally referred to as 'celadonite' in mineralogical textbooks (*e.g.* Bernard, 1981; Bernard and Rost, 1992). Maybe this classification was only based on the green color of the material and the elemental composition resembling celadonite, especially when comparing the Mg and Fe contents (Table 3). The major components of this green earth collected in Brodce, near Kadaň, are, however, smectites, as was proven by XRD. They have complicated compositions representing structural transition among montmorillonite, nontronite and saponite as indicated by the results of the Greene-Kelly test and IR spectroscopy measurements. According to DRS this smectite has a rather uncommon occupation of octahedral and tetrahedral sheets: some Fe^{3+} is probably placed in tetrahedral sheets and leads to the anionic charge being located in both the octahedral and tetrahedral sheets. The presence of Fe^{3+}_{tetra} in ferrugineous smectites is assumed only if all octahedral sites are occupied by Al^{3+} and Fe^{3+}; in nontronites this excess of Fe is achieved at Fe_2O_3 content >34% (Gates *et al*., 2002). The Fe content in Brodce green earth is, however, much smaller than this value. The tetrahedral Fe^{3+} substitution in clay minerals is probably more common than is

https://doi.org/10.1346/CCMN.2004.0520612 Published online by Cambridge University Press

Table 7. Mössbauer spectroscopic parameters of selected Fe-rich smectites.

Sample	Relative area	IS (mm/s)	QS (mm/s)	BHF (T)	Assignment
Rokle	0.97	0.45	0.23		Fe^{3+}
22 K	0.02	0.47	0.69		Fe^{2+}
	0.01		0 (singlet)		?
Brodce	0.74	0.30	0.33		Fe^{3+}
24 K	0.17	0.52	0.62		Fe^{3+}
	0.08	1.27	1.37		Fe^{2+}
	0.01	0.46	0.05	50	Fe^{3+} oxide
NAu-1	0.10	0.46	0.1	10	goethite
293 K	0.90	0.36	0.21		Fe^{3+}
NAu-2	0.08	0.50	0.16	4	goethite
293 K	0.63	0.36	0.11		Fe^{3+}
	0.17	0.40	0.63		Fe^{3+}
	0.12	0.34	0.36		Fe^{3+}
NG-1	0.04	0.3	−0.2	28	goethite
293 K	0.77	0.3	0.16		Fe^{3+}
	0.18	0.6	0.04		?
	0.01	0.6	0.8		?
NG-1	0.77	0.47	0.21		Fe^{3+}
25 K	0.17	0.62	0 (singlet)		?
	0.03	0.25	0.38		Fe^{3+}
	0.02	0.49	−0.13	50	Fe^{3+} oxide
	0.01	0.36	0.01	48	Fe^{3+} oxide

IS: isomeric shift, QS: quadrupole splitting, BHF: hyperfine splitting (sextets).

frequently considered and conventionally calculated from chemical analysis. Bishop *et al*. (2002), for example, tried to explain greater abundances of tetrahedral Fe by similar polarizing powers of Fe^{3+} and Al^{3+}.

The color of green earths is imparted by a reflectance maximum at ~18,000 cm^{-1} lying between the absorption maxima of bands IV and V. However, there is a striking visual difference between the brownish or yellowish green of Fe^{2+}-poor smectites, and the bluish hue of Fe^{2+}-rich minerals such as glauconite, celadonite or chlorite (Grissom, 1986). With increasing Fe^{2+} content in Fe-containing clay minerals, particularly in micas and chlorite, a relatively strong band III starts to dominate over the band IV (Figure 7). However, although there is a statistically significant correlation between bands I and III and Fe^{2+} content, the corresponding absorption coefficients are not constant and depend on the individual minerals. It could be used as a 'fingerprint' or probe of the Fe-bearing clay mineral. For example, the ratio between the integral intensities of bands III and IV is plotted *vs*. Fe^{2+}/Fe^{3+} content in Figure 7. In smectites the III/IV ratio is close to zero in spite of the presence of some Fe^{2+}, and contrary to IMt-1, glauconite and celadonite, the III/IV ratio is >2 even at moderate Fe^{2+}:Fe^{3+} ratios. This observation could be explained in two ways: either the Fe^{2+} and Fe^{3+} ions prefer to form Fe^{2+}-Fe^{3+} pairs in the mica structure, or the minor Fe^{2+} in samples is present in mineral admixtures other than clay minerals. The only exception in Figure 7 is green earth K17400 containing an admixture of goethite according to voltammetry and XRD. Goethite, which was found as the most common admixture of free Fe oxides in green earths, can eliminate the bluish hue of green micas, and it contributed substantially to band IV.

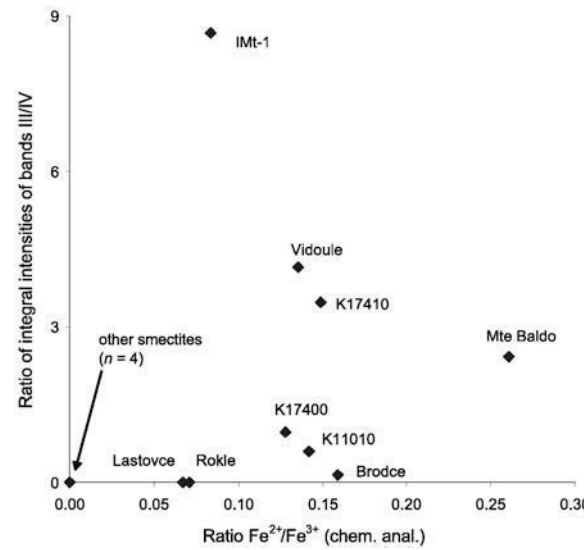

Figure 7. Fingerprint of the clay minerals. The ratio of intervalence charge transfer (IVCT) band III to band IV is plotted against the ratio of divalent and trivalent Fe in the structure. The smectites free of Fe^{2+} are located in point [0,0].

https://doi.org/10.1346/CCMN.2004.0520612 Published online by Cambridge University Press

For the analysis of microsamples containing mineral components, such as paint layers of works of art, light microsocopy, SEM/EDX and in special cases XRD can be applied (Grygar *et al*., 2003b). The easiest means of discriminating between green clay minerals in microsamples is the evaluation of the color and the appearance of particles of green earth. Green micas and possibly chlorites may be present as relatively large particles of bluish green color given by their IVCT. Smectites are, however, inherently nanocrystalline, forming neither concretions nor polycrystalline grains; no estimate of their elemental composition could be made using microanalytical methods such as EDX. Because of its complicated mineralogical composition, Kadaň green smectite resembles green micas in its relatively large Mg and, locally, K content. If only elemental analysis of such a microsample with the green earth pigment is available, smectites formed by alteration of basic volcanic material could probably be indicated by increased Ti content. The relative amount of Ti has already been shown to be suitable in discriminating between yellow and red earths of different origin (Grygar *et al*., 2003b). Both Kadaň green earth and Rokle reference bentonite of volcanogenic origin have an increased Ti content, and the same is valid for the commercially available 'Veronese green earth' (Table 3).

The instrumental method which gives most insight into identification of green earths in microsamples would hence be XRD or similar diffraction micromethod.

CONCLUSIONS

The 'Bohemian' green earth from Brodce does not contain celadonite as a main component, contrary to previous assumptions. The altered volcanogenic material in that locality contains predominantly expandable structures of dioctahedral ferruginous smectite and trioctahedral saponite.

The mica minerals (celadonite, glauconite) and Fe-rich smectites can be distinguished directly by their color properties. The ratios between the bands in the near-IR region (at ~10,000 cm^{-1}) and bands absorbing between 12,000 and 17,000 cm^{-1} can be used to discriminate between smectites and micas in the green earth samples. DRS is a sensitive tool for speciation of Fe in Fe-bearing clay minerals at Fe content >1% and was also found to be more suitable for identifying tetrahedral Fe^{3+} in smectites than was Mössbauer spectroscopy.

The mineralogical classification of greenish smectites is not easy. In all three studied smectite samples ('Veronese' green earths K11010, 'Bohemian' green earth from Brodce, and bentonite from Rokle) the tetrahedrally coordinated Fe was found by DRS. Tetrahedral substitutions explain the 'non-montmorillonitic' behavior (*e.g.* the residual charge and expandability after Li saturation and heating) of samples, which are not true nontronites because of a relatively smaller total Fe content in their structure.

ACKNOWLEDGMENTS

The authors thank Jana Madejová and Helena Palková, Institute of Inorganic Chemistry, Slovak Academy of Sciences, Bratislava, Slovakia, for FTIR measurements and their help with interpretations of results, Kateřina Novotná, Charles University, Prague, Czech Republic, for help with DRS measurements and Veronika Šímová for help with SEM/EDX measurements. Financial support from the Ministry of Education of the Czech Republic (project number LN00A028) and from the Grant agency of the Academy of Sciences of the Czech Republic (project number IAA3032401) is acknowledged.

REFERENCES

Albrecht, E., Ehmig, G. and Barisany, J. (1903) *Das Kaadner Grün – Buchdruckerei Wenzel Hönl*. Kaaden, Germany.

Bernard, J.H. (1981) *Minerals of the Czech Republic – a Brief Review.* Academia, Prague (in Czech).

Bernard, J.H. and Rost, R. (1992) *Encyclopaedia of Minerals*. Academia, Prague (in Czech).

Bílek, J., Jangl, L. and Urban, J. (1976) *The History of Mining in Chomutov region*. Local Museum in Chomutov, Czech Republic, 191 pp. (in Czech).

Bishop, J., Murad, E. and Dyar, M.D. (2002) The influence of octahedral and tetrahedral cation substitution on the structure of smectites and serpentines as observed through infrared spectroscopy. *Clay Minerals*, **37**, 617–628.

Bláhová, A. (2002) The Green Earth from Kadaň. BSc thesis, Faculty of Science, Charles University, Prague, 34 pp. (in Czech).

Bonnin, D., Calas, G., Suquet, H. and Pezerat, H. (1985) Site occupancy in Garfield Nontronite: A spectroscopic study. *Physics and Chemistry of Minerals*, **12**, 55–64.

Cracium, C. (1986) Influence of Fe3+ for Al3+ octahedral substitutions on the IR spectra of montmorillonite minerals. *Spectroscopic Letters*, **17**, 579–590.

Daniila, S., Bikiaris, D., Burgio, L., Gavala, P., Clark, R.J.H. and Chryssoulakis, Y. (2002) An extensive non-destructive and micro-spectroscopic study of two Byzantine overpainted icons of the 16th century. *Journal of Raman Spectroscopy*, **33**, 807–814.

Dyar, M.D. (2002) Optical and Mössbauer spectroscopy of iron in micas. Pp. 313–349 in: *Micas: Crystal Chemistry and Metamorphic Petrology* (A. Mottana, F.P. Sassi, J.B. Thompson and S. Guggenheim, editors). Reviews in Mineralogy and Geochemistry, **46**, Mineralogical Society of America, Washington, D.C.

Fialips, C.-I., Huo, D., Yan, L., Wu, J. and Stucki, J.W. (2002) Effect of Fe oxidation state on the IR spectra of Garfield nontronite. *American Mineralogist*, **87**, 630–641.

Frost, R.L., Kloprogge, J.T. and Ding, Z. (2002) Near-infrared spectroscopic study of nontronites and ferruginous smectite. *Spectrochimica Acta Part A*, **58**, 1657–1668.

Gates, W.P. (in press) Infrared spectroscopy and the chemistry of dioctahedral smectites. In: *The Application of Vibrational Spectroscopy to Clay Minerals and Layered Double Hydroxides* (T. Kloprogge, editor). CMS Workshop Lectures, **13**. Clay Minerals Society, Denver, Colorado.

Gates, W.P., Slade, P.G., Manceau, A. and Lanson, B. (2002) Site occupancies by iron in nontronites. *Clays and Clay Minerals*, **50**, 223–239.

Goodman, B.A., Russell, J.D., Fraser, A.R. and Woodhams, F.W.D. (1976) A Mössbauer and I.R. spectroscopic study of the structure of nontronite. *Clays and Clay Minerals*, **24**, 53–59.

Greene-Kelly, R. (1953) The identification of montmorillonoids in clays. *Journal of Soil Science*, **4**, 233–237.

Grissom, C.A. (1986) Green Earth. In: *Artists Pigments, vol. 1* (L. Feller, editor), Cambridge University Press, Cambridge, UK.

Grygar, T. and van Oorschot, I.H.M. (2002) Voltammetric identification of pedogenic iron oxides in paleosol and loess. *Electroanalysis*, **14**, 339–344.

Grygar, T., Dědeček, J. and Hradil, D. (2002) Analysis of low concentration of free ferric oxides in clays by vis diffuse reflectance spectroscopy and voltammetry. *Geologica Carpathica*, 53, 71–77.

Grygar, T., Dědeček, J., Kruiver, P., Dekkers, M.J., Bezdička, P. and Schneeweiss, O. (2003a) Iron oxide mineralogy in Late Miocene red beds from La Gloria, Spain: Rock-magnetic, Voltammetric and Vis Spectroscopy Analyses. *Catena*, **53**, 115–132.

Grygar, T., Hradilová, J., Hradil, D., Bezdička, P. and Bakardjieva, S. (2003b) Analysis of earthy pigments in grounds of Baroque paintings. *Analytical and Bioanalytical Chemistry*, **375**, 1154–1160.

Hradil, D., Grygar, T., Hradilová, J. and Bezdička, P. (2003) Clay and iron oxide pigments in the history of painting. *Applied Clay Science*, **22**, 223–236.

Keeling, J.L., Raven, M.D. and Gates, W.P. (2000) Geology and characterization of two hydrothermal nontronites from weathered metamorphic rocks at the Uley Graphite Mine, South Australia. *Clays and Clay Minerals*, **48**, 537–548.

Koester, H.M., Ehrlicher, U., Gilg, H.A., Jordan, R., Murad, E. and Onnich, K. (1999) Mineralogical and chemical characteristics of five nontronites and Fe-rich smectites. *Clay Minerals*, **34**, 579–599.

Komadel, P., Lear, P.R. and Stucki, J.W. (1990) Reduction and reoxidation of nontronites: Extent of reduction and reaction rates. *Clays and Clay Minerals*, **38**, 203–208.

Lear, P.R. and Stucki, J.W. (1987) Intervalence electron transfer and magnetic exchange in reduced nontronite. *Clays and Clay Minerals*, **35**, 373–378.

Madejová, J. and Komadel, P. (2001) Baseline studies of The Clay Minerals Society Source Clays: infrared methods. *Clays and Clay Minerals*, **49**, 410–432.

Madejová, J., Komadel, P. and Čičel, B. (1994) Infrared study of octahedral site populations in smectites. *Clay Minerals*, **29**, 319–326.

Malkovský, M. (1985) *Geology of the North-Bohemian Brown Coal Basin and its Surrounding*. ÚÚG, Prague, 424 pp. (in Czech).

Malla, P.B. and Douglas, L.A. (1987) Problems in the identification of montmorillonite and beidellite. *Clays and Clay Minerals*, **35**, 232–236.

Malengreau, N., Muller, J.-P. and Calas, G. (1994) Fe speciation in kaolins: diffuse reflectance study. *Clays and Clay Minerals*, **42**, 137–147.

Manceau, A., Drits, V.A., Lanson, B., Chateigner, D., Wu, J., Huo, D., Gates, W.P. and Stucki, J.W. (2000) Oxidation-reduction mechanisms of iron in dioctahedral smectites: II. Crystal Chemistry of reduced Garfield nontronite. *American Mineralogist*, **85**, 153–172.

Moore, D.M. and Reynolds, R.C. (1997) *X-ray Diffraction and the Identification and Analysis of Clay Minerals*. Oxford University Press, Oxford, UK.

Mosk, J.A. (1975) Analytical methods applied in the investigation of the Bardwell samples, appendix to 'Thomas Bardwell and his practice of painting'. *Studies in Conservation*, **20**, 103–107.

Murad, E. and Wagner, U. (1994) The Mössbauer spectrum of illite. *Clay Minerals*, **29**, 1–10.

Odom, E. (1984) Glauconite and celadonite minerals. Pp. 545–572 in: *Micas* (S.W. Bailey, editor). Reviews in Mineralogy, **13**. Mineralogical Society of America, Washington, D.C.

Scheinost, A.C., Chavernas, A., Barrón V. and Torrent, J. (1998) Use and limitations of second-derivative diffuse reflectance spectroscopy in the visible to near-infrared range to identify and quantify Fe oxide minerals in soils. *Clays and Clay Minerals*, **46**, 528–536.

Sherman, D.M. (1985) The electronic structures of Fe^{3+} coordination sites in iron oxides; applications to spectra, bonding, and magnetism. *Physics and Chemistry of Minerals*, **12**, 161–175.

Sherman, D.M. (1987) Molecular orbital (SCF-Xα-SW) theory of metal-metal charge transfer process in minerals. *Physics and Chemistry of Minerals*, **14**, 355–363.

Sherman, D.M. and Waite, T.D. (1985) Electronic spectra of Fe^{3+} oxides and hydroxide oxides in the near IR to near UV. *American Mineralogist*, **70**, 1262–1269.

Sherman, D.M. and Vergo, N. (1988) Optical (diffuse reflectance) and Mössbauer spectroscopic study of nontronite and related Fe-bearing smectites. *American Mineralogist*, **73**, 1346–1354.

Środoń, J., Drits, V.A., McCarty, D.K., Hsieh, J.C.C. and Eberl, D.D. (2001) Quantitative X-ray diffraction analysis of clay-bearing rocks from random preparations. *Clays and Clay Minerals*, **49**, 514–528.

Vantelon, D., Pelletier, M., Michot, L.J., Barres, O. and Thomas, F. (2001) Fe, Mg and Al distribution in the octahedral sheet of montmorillonites. An infrared study in the OH-bending region. *Clay Minerals*, **36**, 369–379.

Yamasaki, K. and Emoto, Y. (1979) Pigments used on Japanese paintings from the protohistoric period through the 19th century. *Ars Orientalis*, **11**, 1–14.

Zahálka, B. (1921) *On Commercial Compounds of Raw Materials*. Věda přírodní, Prague (in Czech).

(*Received 6 February 2004; revised 24 July 2004; Ms. 881*)